PCCP

COMMUNICATION

View Article Online
View Journal | View Issue

Cite this: *Phys. Chem. Chem. Phys.*, 2016, **18**, 12423

Received 7th March 2016,
Accepted 12th April 2016

DOI: 10.1039/c6cp01553k

www.rsc.org/pccp

Sequential detection of multiple phase transitions in model biological membranes using a red-emitting conjugated polyelectrolyte†

Judith E. Houston,[a] Mario Kraft,[b] Ullrich Scherf[b] and Rachel C. Evans*[a]

The anionic conjugated polyelectrolyte, poly[3-(6-sulfothioatehexyl)-thiophene] (P3Anionic), functions as a highly sensitive probe of membrane order, uniquely capable of sequentially detecting the three key phase transitions occurring within model phospholipid bilayers. The observed sensitivity is the result of charge-mediated, selective localisation of P3Anionic within the head-groups of the phospholipid bilayer.

Cell membranes are complex dynamic systems that modify their structure or phase in order to accomplish different tasks. Membrane phase transitions are crucial for the transport of materials, energy and information between the interior and exterior cell environment.[1] However, membrane order is a delicate balance, and unsought changes in membrane permeability *via* phase transitions are thought to be behind a number of degenerative or life-threatening diseases, including age-related neurological conditions, such as Alzheimer's or Parkinson's disease,[2,3] and tumour cell formation.[4] As such, the development of probes that are able to accurately detect subtle changes in phase or order in model and live membranes at the nanoscale is crucial for the development of targeted diagnostic and therapeutic platforms.[5,6]

Cell membrane order can be probed directly using Raman,[7] optical[8] and atomic force microscopies (AFM).[9] However, these methods often require a fixation procedure, which can introduce artefacts into the images. Indirect methods, such as X-ray and neutron scattering,[10,11] differential scanning calorimetry (DSC)[12,13] and computer simulations[14] allow the cell membrane to be studied in solution, but are not always applicable to *in vivo* measurements. Fluorescent probes overcome these limitations, offering a non-invasive approach to investigate cell membrane order *in vivo* with high sensitivity, low concentration demands and suitable time resolution.[15–21] However, while phase-sensitive fluorescence probes exist (*e.g.* quantum dots,[22] phospholipid labels/analogues,[20,23] small organic dyes[16,24]), their widespread use has been limited by time-consuming experimental procedures, intrinsic cytotoxicity or the tendency towards aggregation or cell internalisation.[25] In contrast, conjugated oligo-/polyelectrolytes (COEs/CPEs) have recently shown considerable promise as lipid phase-transition probes due to their tunable emission, low cytotoxicity and intense fluorescence.[5,26,27] The COEs/CPEs probes reported to date typically show a change in their fluorescence properties in response to a significant membrane transition. The main transition between the liquid-disordered (fluid) and the solid-ordered (gel) phases in lipid bilayers has been shown to induce a red-shift of up to 140 nm in the fluorescence spectra of twisted quarterthiophenes[27] and dithienothiophenes,[5] partly attributed to the planarisation of the oligopolymer backbones within the ordered gel phase. The steady-state emission intensity of the blue-emitting, cationic polyfluorene, HTMA-PFP, was found to be sensitive to two phase transitions in the phospholipids dipalmitoylphosphatidylcholine (DPPC) and 1,2-dimyristoyl-*sn-glycero*-3-phosphocholine (DMPC).[26] In these examples, the COE/CPE probe is able to monitor one, or at most two, membrane transitions *via* its optical properties. Moreover, to the best of our knowledge, there is no COE/CPE probe reported to date that is able to detect the less energetically demanding liquid crystal to lamellar gel transformation, known as the sub-transition, T_s.[28]

Here, we report for the first time a red-emitting, anionic poly(thiophene) CPE, poly[3-(6-sulfothioatehexyl)thiophene], that can be used to sequentially monitor the three primary phase transitions in model lipid cell membranes using a single probe. **P3Anionic** (M_n = 4990 g mol^{-1}, PDI = 1.13) was synthesised as previously reported (Fig. 1a).[29,30] The CPE contains one charge per repeat unit (r.u.) and is soluble in water at pH = 7.3. The zwitterionic phospholipid **DPPC** (Fig. 1a) was prepared as large unilamellar vesicles (LUVs) in HEPES buffer solution (pH = 7.3, 30 mM NaCl) as a model cell membrane. **DPPC** was selected as

[a] *School of Chemistry, University of Dublin, Trinity College, College Green, Dublin 2, Ireland. E-mail: raevans@tcd.ie*
[b] *Macromolecular Chemistry Group (buwmacro) and Institute for Polymer Technology, Bergische Universität Wuppertal, D-42119, Wuppertal, Germany*

† Electronic supplementary information (ESI) available: Synthesis of **P3Anionic**, preparation of **DPPC** vesicles, instrumental methods, fluorescence, representative correlogram and phase diagram for DLS and ζ, respectively, DLS data, DSC thermograms and AFM images. See DOI: 10.1039/c6cp01553k

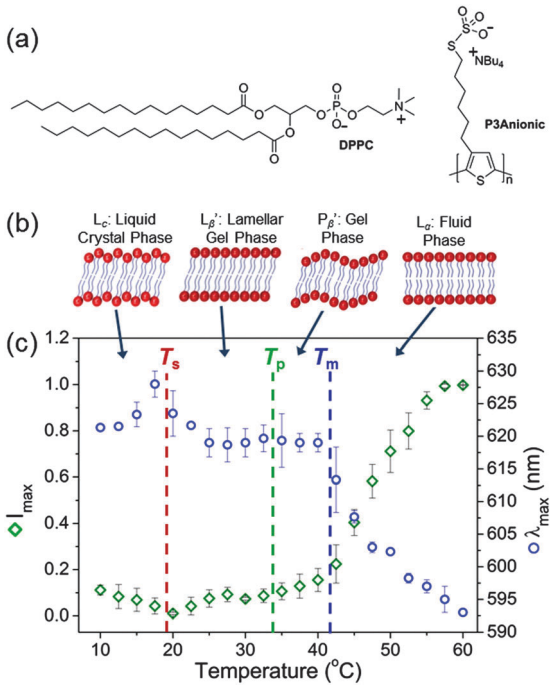

Fig. 1 (a) Chemical structures of the phospholipid, **DPPC**, and the polythiophene, **P3Anionic**. (b) Schematic representations of the expected structure of the bilayer phases at different temperatures. (c) Temperature dependence of the maximum emission intensity (green diamonds) and the emission maximum, λ_{max} (blue circles) of **P3Anionic–DPPC** at 2.0×10^{-5} M (r.u.). The dashed lines indicate the sub- (T_s), pre- (T_p) and main transition temperatures (T_m).

it undergoes three distinct phase transitions, as shown in Fig. 1b: (i) sub-transition between the liquid crystal, L_c, and lamellar gel, L_β', phases (~19 °C),[31] (ii) pre-transition between the L_β' and gel, P_β', phases (32–35 °C)[13] and (iii) main transition between the P_β' and fluid, L_α, phases (~42 °C).[31] For each measurement, stock solutions of the CPE were mixed with stock solutions of the **DPPC** LUVs in HEPES buffer to obtain the required charge ratio between the negative **P3Anionic** monomer units and the zwitterionic **DPPC** molecules.

In order to establish the sensitivity of **P3Anionic** to membrane order, the temperature dependence of the fluorescence properties of the **P3Anionic–DPPC** complex were monitored (Fig. 1c). Dilute samples of the CPE and CPE : **DPPC** mixture at a 1 : 1 charge ratio were measured at 2.5 °C intervals between 10–60 °C. Three distinct changes were noted in the emission spectra in response to the temperature: (i) an increase in the emission maximum, λ_{max}, and a decrease in emission intensity between 17.5–20 °C, corresponding to the sub-transition temperature (T_s) at 18.8 °C;[31] (ii) an increase in the emission intensity above 32.5 °C, which corresponds to the pre-transition temperature (T_p) of **DPPC** (at 32–35 °C);[13] (iii) the λ_{max} blue-shifts rapidly above 40 °C, which corresponds to the main phase transition temperature (T_m) of 41.6 °C between the gel and fluid phase.[31] The observed emission intensity enhancement and blue-shift in the λ_{max} are indicative of higher interchain disorder due to distortion of the thienylene building blocks, which leads to a corresponding decreased conjugative interaction in the deaggregated state.[32–34] This suggests that **P3Anionic** is located in a motionally restricted environment within the lipid bilayer.[35,36] This response mode contrasts that of some other microenvironment fluorescent probes, which distinguish phospholipid phases by the penetration depth of water molecules into the lipid bilayer and the degree of lipid packing.[13,15,20,35] It should be noted that after equilibrating the CPE : **DPPC** mixture at 4 °C for a few days, the initial emission intensity and λ_{max} were recovered. In contrast, the emission intensity of pure **P3Anionic** in HEPES buffer decreased proportionately as the temperature was increased over this range (Fig. S3, ESI†).

To confirm that the observed changes in the fluorescence spectrum as a function of temperature correspond to the phase transitions of pure **DPPC**, DSC measurements were performed on the LUVs before and after the addition of **P3Anionic** (Fig. S4, ESI†). The T_m gave rise to an intense, sharp peak at ~42 °C,[13] the T_p is a less intense broad peak at 31–33 °C,[13] whilst the T_s is not observed in the thermogram, which is common for lipid bilayers.[28] This confirms that the phase transitions specific to **DPPC** are retained upon addition of the CPE and correlate well with the observed spectral changes. In addition, the negligible effect on the shape or position of the T_m profile at ~41 °C upon addition of **P3Anionic** signifies the absence of any substantial lipid reorganisation due to CPE binding.[12] However, an increase in the width of the peaks may suggest a decrease in cooperativity among the acyl chains of the **DPPC** bilayers,[37] whilst the modest decrease in the pre-transition temperature ($\Delta T_p \approx -2$ °C) can be attributed to slight destabilisation of the ordered bilayers.[38] One possible explanation for this effect is that CPE incorporation disrupts the van der Waals forces between **DPPC** molecules.[26] Although subtle, these apparent structural rearrangements may confer an undesirable increase in the permeability of the membrane bilayer[39] or limit the potential resolution of the phase transition temperatures acquired using this method to within a few degrees Celsius.

Phase transition probes require specific localisation of the probe within the phospholipid hydrophobic tails and/or hydrophilic head-groups.[5,35] Considering the chemical structures, electrostatic association between the anionic CPE and the positive-charge on the zwitterionic phospholipid head-group is expected.[40] The UV/vis absorption and fluorescence spectra of **P3Anionic** were studied as a function of the concentration of **DPPC** vesicles at 25 °C. Titration of **DPPC** LUVs into a dilute solution of **P3Anionic** (1.93×10^{-5} M (r.u.)) resulted in a significant blue-shift and increased absorbance of the CPE ($\Delta\lambda_{abs}$ = 435–425 nm), which is accompanied by a red-edge broadening, as shown in Fig. 2a. Red-edge broadening has previously been attributed to an increase in the conjugation length of the CPE;[34,41–43] however scattering effects arising from the addition of nanometre sized vesicles to the solution cannot be excluded. **P3Anionic** exhibits a single broad emission band (λ_{max} = 607 nm) which is quenched upon the addition of **DPPC** LUVs (Fig. 2b). The amplified quenching of the **P3Anionic** emission by **DPPC** vesicles could be the result of the CPE embedding within the membrane and forming non-emissive ground-state complexes with the charged phospholipid head-groups.[42]

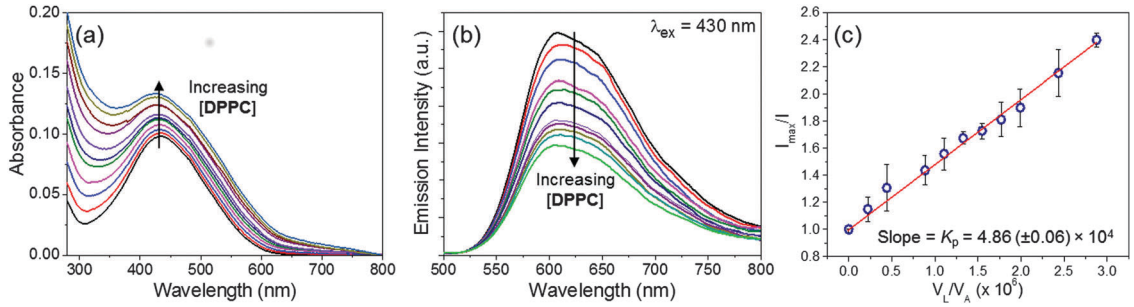

Fig. 2 (a) UV/vis absorption and (b) fluorescence spectra of **P3Anionic** (1.93 × 10^{-5} M (r.u.)) titrated with **DPPC** vesicles (0–4.08 × 10^{-5} M) in pH 7.3 HEPES buffer (30 mM NaCl). (c) Plot of I_{max}/I *vs.* lipid volume fraction to determine the partition coefficient, K_p.

The partition coefficient, K_p, provides information about the partitioning of the CPE between the lipid and water phases of the phospholipid vesicles, and can be determined from the quenching of the fluorescence intensity, from:[44]

$$\frac{I_{max}}{I} = 1 + K_p\alpha \quad (1)$$

where I_{max} is the initial intensity, α is V_L/V_w and V_L is the volume of lipid and V_w is the total volume. V_L can be calculated by taking the volume of a **DPPC** molecule as 1148 Å^3.[45] The plot of I_{max}/I *vs.* α should yield a linear plot where the slope is equal to K_p, as shown in Fig. 2c for **P3Anionic**. The large K_p value (4.86 (±0.06) × 10^4) implies that the CPE is buried within the charged head groups of the bilayer, and not simply coating the vesicle surface.

Dynamic light scattering (DLS) has previously been used to confirm that the integrity of phospholipid vesicles is retained upon the addition of a CPE.[46] The *z*-average hydrodynamic diameter (D_h) of the **DPPC** vesicles was measured before and after addition of **P3Anionic**.[47] The D_h of the **DPPC** vesicles was 115.3 (±2.0) nm with a narrow polydispersity (PDI) of 0.12 (±0.01). The D_h of the pure CPE was 244.7 (±2.5) nm. The **DPPC** vesicle size increased to 130.0 (±4.5) nm for **DPPC–P3Anionic** (1 : 1 charge ratio), indicating that the vesicle structure is not disrupted into smaller fragments,[46] and that no polymer aggregates are formed.[48] In addition, the PDI only increases slightly to 0.16 (±0.02), significantly lower than that of the pure CPE at ∼0.3. Zeta potential (ζ) measurements can be used to determine the effective charge of the vesicle surface, which will change depending on whether electrostatic association between the CPE and **DPPC** occur at the vesicle surface or within the lipid bilayer.[49] In HEPES buffer (pH 7.3) **P3Anionic** exhibits a negative ζ of −28.1 (±5.2) mV, whilst the ζ of the **DPPC** LUVs was −3.3 (±0.1) mV, which is close to the literature value of ∼−4.4 mV.[50] Upon addition of **P3Anionic** to a solution of **DPPC** LUVs (1 : 1), the ζ decreased significantly to −25.4 (±1.0) mV. Since the **DPPC** vesicles do not completely adopt the ζ of **P3Anionic**, this suggests that the CPE may be partially penetrating the lipid bilayer, which shields some of the charge, whilst some chains protrude from the outer surface.[51]

Epi-fluorescence microscopy was performed on a mixture of **P3Anionic**/**DPPC** multilamellar vesicles (MLVs)[52] to demonstrate whether **P3Anionic** is an effective fluorescent membrane marker (Fig. 3a). The vesicle structure is clearly observable, with the CPE emission localising on the outer layers of the MLVs, demonstrating that the CPE is not internalised within the vesicle. AFM was then used to study the surface morphology of **P3Anionic–DPPC** LUVs. Samples were found to contain features of two population sizes.[53] Small spherical objects, ∼70 nm in diameter, were observed, which are assigned to undoped vesicles (Fig. S7, ESI†). There is no evidence of the pure CPE aggregates which formed large, amorphous aggregates (Fig. S8, ESI†). The second population of objects in the **P3Anionic–DPPC** samples were 158 (±78) nm in diameter (Fig. 3b). The inset in Fig. 3b clearly shows a multilayer structure in these objects. The inner spheres have a diameter of ∼120 nm, while the outer shell could be CPE protruding from the vesicle surface as suggested by ζ measurements.

The global results indicate a distinct assembly pattern for the **P3Anionic–DPPC** associations, as shown by the scheme in Fig. 3c.

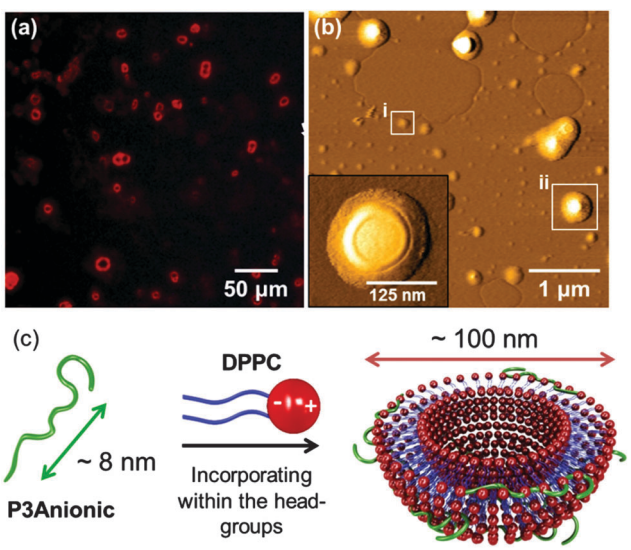

Fig. 3 (a) Epi-fluorescence images of **DPPC** multilamellar vesicles (MLV) (2.6 × 10^{-3} M) titrated with **P3Anionic** (1.3 × 10^{-3} M (r.u.)), λ_{ex} = 435 nm. (b) AFM tapping mode images of **P3Anionic–DPPC** at 1 : 1 charge ratio (2.0 × 10^{-5} M): (i) undoped **DPPC** vesicle, (ii) **P3Anionic**-doped vesicle. Inset: Superfine image of doped vesicle structure. (c) Schematic representation of the proposed self-assembly mechanism of **P3Anionic** with zwitterionic **DPPC** vesicles.

The changes in the UV/vis absorption and fluorescence spectra confirm electrostatic interaction between **P3Anionic** and **DPPC** vesicles. AFM, Epi-fluorescence and zeta potential measurements suggest that **P3Anionic** penetrates within the head-groups of the lipid bilayer, with some chains protruding from the surface. We propose that the net negative charge on **P3Anionic** works two-fold to control the localisation of the poly(thiophene) within the phospholipid bilayer. Firstly, electrostatic attraction with the external positive ammonium ion of the **DPPC** may draw the CPE within the head-group region of the bilayer. However, concomitantly electrostatic and hydrophobic–hydrophilic repulsive forces will exist between the negatively charged **P3Anionic** and the sulfonate group on **DPPC** and the hydrophobic phospholipid tails, respectively, preventing **P3Anionic** from burying deeper within the **DPPC** bilayer. The specific localisation within the head-group region where the CPE will be motionally restricted[35] and thus sensitive to the phase of the lipid bilayer, as we have observed.

Recently, drug delivery systems based on phospholipid unilamellar vesicles have been realised which undergo thermally-triggered phase transformations from the gel to the more permeable liquid phase, stimulating the release of the encapsulated drug.[54] The unique ability of **P3Anionic** to monitor phase transitions in real time thus presents a significant opportunity for the development of targeted theranostic platforms based on synthetic zwitterionic phospholipids. Furthermore, as zwitterionic phospholipids form the major component of real cell membranes, we anticipate the observed localisation of **P3Anionic**, and its sensitivity to phase transitions, to be reflected in real cell membrane studies. However, it should be noted that this study utilises a simplified membrane system, that does not include the multitude of other lipid molecules present in membranes including sphingolipids, cholesterol and membrane proteins.[1] These molecules will affect the localisation of the poly(thiophene) within the lipid bilayers to an unknown extent. Thus, whilst this preliminary study has focused on a model membrane system to highlight the effectiveness of **P3Anionic** as a membrane order probe, future efforts will determine whether **P3Anionic** can be implanted successfully in live cells.

In summary, we have demonstrated that the red-emitting poly(thiophene), **P3Anionic**, functions as a fluorescent probe for the sequential identification of the three key phase transitions occurring within **DPPC** bilayers. In particular, we have shown a facile method to determine the illusive sub-transition temperature of phospholipid membranes. The anionic CPE undergoes charge-mediated localisation within the zwitterionic head-group region of the lipid bilayers where the sensitivity to membrane order is believed to be the greatest.[35] Moreover, the large polymer size is known to inhibit cell internalisation,[37] which is a common problem for small molecule fluorescent dyes.[25] Whilst at only 8 nm in length, **P3Anionic** remains small enough to accurately probe the raft-like nanodomains in cell membranes (10–200 nm), whose role and impact in cell function is yet to be fully understood.[2,4,55] Finally, due its emission in the far-red region **P3Anionic** should be an ideal probe for *in vivo*/*in vitro* studies, since interference from tissue autofluorescence should be minimal.

Acknowledgements

This work was supported by a Trinity Award postgraduate scholarship (J. E. H.). The authors would like to thank Dr Gavin McManus for assistance with epi-fluorescence microscopy.

Notes and references

1 R. B. Gennis, *Biomembranes: Molecular Structure and Function*, Springer-Verlag New York, Inc., 1989, pp. 1.
2 R. Marin, J. A. Rojo, N. Fabelo, C. E. Fernandez and M. Diaz, *Neuroscience*, 2013, **245**, 26.
3 N. Fabelo, V. Martín, G. Santpere, R. Marín, L. Torrent, I. Ferrer and M. Díaz, *Mol. Med.*, 2011, **17**, 1107.
4 W. Stillwell and S. R. Wassall, *Chem. Phys. Lipids*, 2003, **126**, 1.
5 M. Dal Molin, Q. Verolet, A. Colom, R. Letrun, E. Derivery, M. Gonzalez-Gaitan, E. Vauthey, A. Roux, N. Sakai and S. Matile, *J. Am. Chem. Soc.*, 2015, **137**, 568.
6 A. S. Klymchenko and R. Kreder, *Chem. Biol.*, 2014, **21**, 97.
7 J. Ando, M. Kinoshita, J. Cui, H. Yamakoshi, K. Dodo, K. Fujita, M. Murata and M. Sodeoka, *Proc. Natl. Acad. Sci. U. S. A.*, 2015, **112**, 4558.
8 R. Dimova, S. Aranda, N. Bezlyepkina, V. Nikolov, K. A. Riske and R. Lipowsky, *J. Phys.: Condens. Matter*, 2006, **18**, S1151.
9 A. Alessandrini and P. Facci, *Soft Matter*, 2014, **10**, 7145.
10 F. A. Heberle, R. S. Petruzielo, J. Pan, P. Drazba, N. Kučerka, R. F. Standaert, G. W. Feigenson and J. Katsaras, *J. Am. Chem. Soc.*, 2013, **135**, 6853.
11 J. Pan, F. A. Heberle, S. Tristram-Nagle, M. Szymanski, M. Koepfinger, J. Katsaras and N. Kučerka, *Biochim. Biophys. Acta*, 2012, **1818**, 2135.
12 A. A. Yaroslavov, T. A. Sitnikova, A. A. Rakhnyanskaya, E. G. Yaroslavova, D. A. Davydov, T. V. Burova, V. Y. Grinberg, L. Shi and F. M. Menger, *J. Am. Chem. Soc.*, 2009, **131**, 1666.
13 K. A. Riske, R. P. Barroso, C. C. Vequi-Suplicy, R. Germano, V. B. Henriques and M. T. Lamy, *Biochim. Biophys. Acta*, 2009, **1788**, 954.
14 S. Baoukina, E. Mendez-Villuendas, W. F. D. Bennett and D. P. Tieleman, *Faraday Discuss.*, 2013, **161**, 63.
15 V. Kilin, O. Glushonkov, L. Herdly, A. Klymchenko, L. Richert and Y. Mely, *Biophys. J.*, 2015, **108**, 2521.
16 M. R. Dent, I. López-Duarte, C. J. Dickson, N. D. Geoghegan, J. M. Cooper, I. R. Gould, R. Krams, J. A. Bull, N. J. Brooks and M. K. Kuimova, *Phys. Chem. Chem. Phys.*, 2015, **17**, 18393.
17 I.-H. Lee, S. Saha, A. Polley, H. Huang, S. Mayor, M. Rao and J. T. Groves, *J. Phys. Chem. B*, 2015, **119**, 4450.
18 R. Kreder, K. A. Pyrshev, Z. Darwich, O. A. Kucherak, Y. Mély and A. S. Klymchenko, *ACS Chem. Biol.*, 2015, **10**, 1435.
19 A. P. Demchenko, Y. Mély, G. Duportail and A. S. Klymchenko, *Biophys. J.*, 2009, **96**, 3461.
20 R. Saxena, S. Shrivastava, S. Haldar, A. S. Klymchenko and A. Chattopadhyay, *Chem. Phys. Lipids*, 2014, **183**, 1.
21 M. Nazari, M. Kurdi and H. Heerklotz, *Biophys. J.*, 2012, **102**, 498.

22 W. Zheng, Y. Liu, A. West, E. E. Schuler, K. Yehl, R. B. Dyer, J. T. Kindt and K. Salaita, *J. Am. Chem. Soc.*, 2014, **136**, 1992.
23 H. Sasaki and S. H. White, *Biophys. J.*, 2009, **96**, 4631.
24 J. Seeliger, N. Erwin, C. Rosin, M. Kahse, K. Weise and R. Winter, *Phys. Chem. Chem. Phys.*, 2015, **17**, 7507.
25 H.-Y. Wang, H.-R. Jia, X. Lu, B. Chen, G. Zhou, N. He, Z. Chen and F.-G. Wu, *J. Mater. Chem. B*, 2015, **3**, 6165.
26 Z. Kahveci, M. J. Martínez-Tomé, R. Esquembre, R. Mallavia and C. R. Mateo, *Materials*, 2014, **7**, 2120.
27 D. A. Doval, M. Dal Molin, S. Ward, A. Fin, N. Sakai and S. Matile, *Chem. Sci.*, 2014, **5**, 2819.
28 M. Kinoshita, K. Ito and S. Kato, *Chem. Phys. Lipids*, 2010, **163**, 712.
29 M. Kraft, S. Adamczyk, A. Polywka, K. Zilberberg, C. Weijtens, J. Meyer, P. Görrn, T. Riedl and U. Scherf, *ACS Appl. Mater. Interfaces*, 2014, **6**, 11758.
30 For full synthetic procedure of **P3Anionic** see the ESI†.
31 R. Koynova and M. Caffrey, *Biochim. Biophys. Acta*, 1998, **1376**, 91.
32 K. K. Stokes, K. Heuzé and R. D. McCullough, *Macromolecules*, 2003, **36**, 7114.
33 C. Tan, E. Atas, J. G. Müller, M. R. Pinto, V. D. Kleiman and K. S. Schanze, *J. Am. Chem. Soc.*, 2004, **126**, 13685.
34 R. C. Evans, M. Knaapila, N. Willis-Fox, M. Kraft, A. Terry, H. D. Burrows and U. Scherf, *Langmuir*, 2012, **28**, 12348.
35 S. Shrivastava, S. Haldar, G. Gimpl and A. Chattopadhyay, *J. Phys. Chem. B*, 2009, **113**, 4475.
36 It is known that the labile sulfur–sulfur bonds of the anionic thiosulfate groups can undergo decomposition under thiol formation followed by further chemical reactions. It can't be fully excluded that the CPEs are to some extent anchored into the lipid bilayers by covalent chemical bonding.
37 M. J. Tapia, M. Monteserín, H. D. Burrows, J. A. S. Almeida, A. A. C. C. Pais, J. Pina, J. S. Seixas de Melo, S. Jarmelo and J. Estelrich, *Soft Matter*, 2015, **11**, 303.
38 V. Librando, M. G. Sarpietro and F. Castelli, *Environ. Toxicol. Pharmacol.*, 2003, **14**, 25.
39 S. Drori, G. D. Eytan and Y. G. Assaraf, *Eur. J. Biochem.*, 1995, **228**, 1020.
40 T. Costa, D. de Azevedo, B. Stewart, M. Knaapila, A. J. M. Valente, M. Kraft, U. Scherf and H. D. Burrows, *Polym. Chem.*, 2015, **6**, 8036.
41 T. M. Swager, C. J. Gil and M. S. Wrighton, *J. Phys. Chem.*, 1995, **99**, 4886.
42 S. M. Fonseca, R. P. Galvão, H. D. Burrows, A. Gutacker, U. Scherf and G. C. Bazan, *Macromol. Rapid Commun.*, 2013, **34**, 717.
43 M. Chevrier, J. E. Houston, J. Kesters, N. Van den Brande, A. E. Terry, S. Richeter, A. Mehdi, O. Coulembier, P. Dubois, R. Lazzaroni, B. Van Mele, W. Maes, R. C. Evans and S. Clément, *J. Mater. Chem. A*, 2015, **3**, 23905.
44 M. Vermeir, N. Boens and K. P. Heirwegh, *Biochem. J.*, 1992, **284**, 483.
45 A. I. Greenwood, S. Tristram-Nagle and J. F. Nagle, *Chem. Phys. Lipids*, 2006, **143**, 1.
46 L. Ding, E. Y. Chi, S. Chemburu, E. Ji, K. S. Schanze, G. P. Lopez and D. G. Whitten, *Langmuir*, 2009, **25**, 13742.
47 A representative correlogram and phase diagram for the DLS and zeta potential measurements, respectively, are available in the ESI†.
48 Z. Kahveci, R. Vázquez-Guilló, M. J. Martínez-Tomé, R. Mallavia and C. R. Mateo, *ACS Appl. Mater. Interfaces*, 2016, **8**, 1958.
49 H. Y. Fan, M. Nazari, G. Raval, Z. Khan, H. Patel and H. Heerklotz, *Biochim. Biophys. Acta*, 2014, **1838**, 2306.
50 A. E. Wiącek, *Appl. Surf. Sci.*, 2011, **257**, 4495.
51 M. Kepczynski, D. Jamróz, M. Wytrwal, J. Bednar, E. Rzad and M. Nowakowska, *Langmuir*, 2012, **28**, 676.
52 Larger MLVs (5–20 μm in diameter) were used for Epi-fluorescence microscopy measurements due to the limited size resolution of this technique. The preparation procedure for MLVs is in the ESI†.
53 Doped and undoped vesicles were assigned according to their relative diameters. Small spheres (~70 nm) were assigned to 'undoped' **DPPC** vesicles based on the average vesicle diameter determined from pure **DPPC** samples, see Fig. S7a, ESI.† Larger spheres (>100 nm) were assigned as **P3Anionic**-doped **DPPC** vesicles.
54 D. Needham, G. Anyarambhatla, G. Kong and M. W. Dewhirst, *Cancer Res.*, 2000, **60**, 1197.
55 D. Lingwood and K. Simons, *Science*, 2010, **327**, 46.